



H₂S conversion in a tubular flow reactor: Experiments and kinetic modeling

J.M. Colom-Díaz^a, M. Abián^a, M.Y. Ballester^b, Á. Millera^a, R. Bilbao^a,
M.U. Alzueta^{a,*}

^a *Aragón Institute of Engineering Research (I3A). Department of Chemical and Environmental Engineering, University of Zaragoza, 50018 Zaragoza, Spain*

^b *Physics Department, Federal University of Juiz de Fora, MG 36036-330, Brasil*

Received 30 November 2017; accepted 25 May 2018

Available online xxx

Abstract

Oxidation of H₂S at atmospheric pressure has been studied under different reaction atmospheres, varying the air excess ratio (λ) from reducing ($\lambda = 0.32$) to oxidizing conditions ($\lambda = 19.46$). The experiments have been carried out in a tubular flow reactor, in the 700–1400 K temperature range. The concentrations of H₂S, SO₂ and H₂ have been determined and the experimental results have been simulated with a detailed chemical mechanism compiled in the present work. The experimental results obtained indicate that H₂S consumption is shifted to lower temperatures as the stoichiometry increases, starting at 925 K for reducing conditions and at 700 K for the most oxidizing ones. The model reproduces well, in general, the experimental data from the present work, and those from the literature at high pressures. Supported by theoretical calculations, the isomerization of HSOO to HSO₂ has been determined as an alternative and possible pathway to the final product SO₂, from the key SH + O₂ reaction.

© 2018 Published by Elsevier Inc. on behalf of The Combustion Institute.

Keywords: H₂S; Oxidation; Sour gas; PFR; Kinetic modeling

1. Introduction

Conventional natural gas, as well as different non-conventional fuel mixtures or biogas generated in anaerobic digestion, may contain different amounts of hydrogen sulfide (H₂S) in their composition. Additionally, hydrogen sulfide can also be found as a by-product from the oil industry, re-

leased from the pyrolysis of fuels containing sulfur, natural gas cleaning or in synthesis gas produced from gasification of coal and biomass. Due to the corrosive and harmful nature of hydrogen sulfide, streams containing H₂S are led to cleaning treatments (e.g., amine absorption) and sulfur recovery units, which convert hydrogen sulfide into sulfur through the Claus process. This process is divided in two reaction steps: in the first one (thermal step), H₂S undergoes a partial oxidation in air, and then in the second one, it reacts with SO₂ to form sulfur in the presence of a catalyst (catalytic step) [1–3].

* Corresponding author.

E-mail address: uxue@unizar.es (M.U. Alzueta).

<https://doi.org/10.1016/j.proci.2018.05.005>

1540-7489 © 2018 Published by Elsevier Inc. on behalf of The Combustion Institute.

As the energy demand increases worldwide, an efficient utilization of available natural resources is needed. The increasing importance of fuel sources, such as sour and shale gas (up to 30% of hydrogen sulfide content in volume), brings interest to the direct use of these fuels without the use of expensive cleaning treatments and to devote the main effort to the development of technologies and combustion processes [4]. The different fuel compositions, together with the presence of different combustion atmospheres, may affect the conversion of H_2S . In this context, it is interesting to be able to predict the most appropriate conditions for stable combustion at the desired temperatures, with minor pollutant emissions.

However, the oxidation steps chemistry of H_2S remains unknown in many aspects, and the available experimental data are limited. In 2000, Gardiner et al. [5] reviewed the significant progress in the understanding of the kinetics and mechanisms of the atmospheric oxidation chemistry of sulfur in the last decades, indicating the less effort placed on developing and understanding sulfur combustion kinetics. More recent studies have faced different combustions chemistry studies. For example, Bongartz and Ghoniem [6] developed an optimized mechanism to make predictions on the combustion behavior of sour gas under oxy-fuel conditions. In the same way, Cong et al. [2] developed a mechanism to assess the production of hydrogen through H_2S thermolysis for the Claus process. Despite these efforts, there is still a need for more accurate direct determination of several important rate constants as well as more validation data [6].

Additionally, there are also experimental works involving H_2S oxidation. For example, earlier investigations at high temperatures [7], H_2S mixtures explosion limit determinations [8], induction time measurements in reflected shock waves [9] or premixed flames [10], have been performed. Besides, recent researches in flow reactors, more related to this study, include the work of Zhou et al. [11], who performed experiments of H_2S oxidation in a flow reactor at atmospheric pressure, under fuel-lean conditions and in the temperature range of 950–1150 K. In another study, Song et al. [12] conducted experiments at high pressures (30–100 bar), evaluating the oxidation of H_2S under oxidizing and stoichiometric conditions, concluding that the combustion behavior depends strongly on the stoichiometry and pressure.

In this context, the present study aims to extend the results available in the literature related to H_2S conversion, and addresses the oxidation of H_2S under different stoichiometries, ranging from fuel-rich to fuel lean conditions. Experimental work in a tubular flow reactor at atmospheric pressure has been performed, in the temperature range of 700–1400 K. A kinetic model developed by our group, updated for this work, has been used to simulate the experimental results.

2. Experimental methodology

The experiments have been carried out in a quartz tubular flow reactor at atmospheric pressure. Only a brief experimental setup description is given here and a more detailed description can be found elsewhere [13]. The reactor has a reaction zone of 20 cm in length and 0.87 cm of internal diameter. Total flow rate in all experiments was 1 L (STP)/min, resulting in a gas residence time as a function of temperature of $194.6/T(\text{K})$, in seconds. The reactor is placed in a three-zone electrically heated oven, ensuring a uniform temperature profile (± 5 K) along the reaction zone. Besides, heat release from chemical reactions is minimized by performing the experiments under highly diluted conditions and using nitrogen to balance. Gases from gas cylinders are led to the reactor in up to four separate streams, which are heated separately and mixed in cross flow at the reactor inlet. At the outlet of the reaction zone, using an external cooling air, the product gas is quenched. The flue gases are led to the analysis system previous pass through a condenser and a filter, that remove any possible residual solid and moisture, therefore a constant supply of clean dry combustion gases is delivered to the analyzers. The analysis instrumentation consists of a UV continuous analyzer for sulfur dioxide (SO_2) concentration measurements and a gas micro-chromatograph for H_2S and H_2 quantification. The uncertainty of the measurements is estimated within 5%.

3. Kinetic model

The experimental results were interpreted in terms of kinetic modeling, using an updated kinetic model based on earlier works by our group [14–16]. This updated model counted with a sub-set of sulfur chemistry reactions, but it was focused on SO_2 reactions. Therefore, additional hydrogen sulfide reactions have been added, taken mainly from the kinetic model by Song et al. for H_2S oxidation at high pressures [12]. The final reaction mechanism listing is included as supplementary material and can be obtained directly from authors. Modifications made in the present work are denoted as “present work: pw”. As for thermochemical data, same sources as for the corresponding reactions were used. Calculations were carried out in the frame of Chemkin Pro with the PFR model [17].

Hydrogen sulfide reacts primarily with radicals like H, OH or HO_2 to form mainly SH radicals. In general, the reactions of H_2S with the radical pool have been determined either experimental and/or theoretically, and are known with certain confidence. The exception is the $\text{H}_2\text{S} + \text{HO}_2$ reaction, for which only an upper limit for the rate constant at room temperature is available [18]. This reaction has two different

138 product channels: $\text{H}_2\text{S} + \text{HO}_2 \rightleftharpoons \text{SH} + \text{H}_2\text{O}_2$ and
 139 $\text{H}_2\text{S} + \text{HO}_2 \rightleftharpoons \text{HSO} + \text{H}_2\text{O}$. The uncertainty of the
 140 reaction kinetic parameters for the first chan-
 141 nel and its high sensitivity have been previously
 142 mentioned elsewhere, especially in high-pressure
 143 works, where HO_2 radicals are expected to play
 144 a major role [12,19,20]. Scarce data referred to
 145 this reaction are available in the literature. There
 146 is also an experimental determination at room
 147 temperature for the reverse channel producing
 148 $\text{SH} + \text{H}_2\text{O}_2$ [21]. Available theoretical calculations
 149 include those by Zhou et al. [11] for the reversible
 150 $\text{H}_2\text{S} + \text{HO}_2 \rightleftharpoons \text{SH} + \text{H}_2\text{O}_2$ reaction, which was then
 151 lowered by a factor of 2 by Mathieu et al. [20],
 152 and calculations by Batiha et al. [22], indicating a
 153 much lower rate constant value. The recent work of
 154 Gersen et al. [19] on the effect of H_2S addition to
 155 methane ignition and oxidation at high pressures
 156 also identified the $\text{H}_2\text{S} + \text{HO}_2$ reaction to be im-
 157 portant and claimed for the need of an accurate
 158 determination of its rate constant. Calculations in
 159 the present work were very sensitive to this reac-
 160 tion, in particular to the $\text{SH} + \text{H}_2\text{O}_2$ channel, and
 161 thus their kinetic parameters were estimated in the
 162 present work as $5 \cdot 10^{12} \text{ cm}^3/\text{mol s}$ for the reverse re-
 163 action, i.e., $\text{SH} + \text{H}_2\text{O}_2 \rightleftharpoons \text{H}_2\text{S} + \text{HO}_2$. This estima-
 164 tion agrees well with the high temperature data of
 165 Zhou et al. [11] and Mathieu et al. [20], while it
 166 is considerably higher than the value of Friedl et
 167 al. [21], experimentally characterized at 298 K. The
 168 impact of this important reaction is further dis-
 169 cussed in the “Results and discussion” section.

170 H_2S conversion mainly produces SH radicals.
 171 Subsequently such a diatom reacts and interme-
 172 diate species are formed. This is considered as
 173 a key reaction step in the bibliography for H_2S
 174 combustion. Particular attention has been devoted
 175 to the $\text{SH} + \text{O}_2$ reaction [11,12,19,23,24] and sig-
 176 nificant differences concerning the rate constants
 177 and product channels of the $\text{SH} + \text{O}_2$ reaction
 178 have been reported in the literature. Stachnik and
 179 Molina [25] provided an upper limit rate con-
 180 stant for this reaction at 298 K of $2 \cdot 10^5 \text{ cm}^3/\text{mol}$
 181 s. This reaction has been largely studied theo-
 182 retically [11,26–29] and several product channels
 183 have been proposed, i.e., $\text{HSO} + \text{O}$, $\text{S} + \text{HO}_2$, and
 184 $\text{SO} + \text{OH}$.

185 Zhou and coworkers [11], in their atmospheric
 186 pressure study, indicated that the production of
 187 $\text{SO} + \text{OH}$ predominates at temperatures below
 188 1000 K, while the formation of $\text{HSO} + \text{O}$ is the
 189 main pathway above this temperature. As will
 190 be seen later, these reactions are not very im-
 191 portant for the conditions of the present work.
 192 Garrido et al. [26], in a high level ab initio study
 193 of the HSO_2 system, identified a new reaction
 194 channel for the $\text{SH} + \text{O}_2$ reaction, which would
 195 produce the preferred $\text{SO}_2 + \text{H}$ channel, via the
 196 HSO_2 intermediate. Song et al. [12] determined
 197 the kinetic parameters for the $\text{SH} + \text{O}_2 \rightleftharpoons \text{SO}_2 + \text{H}$
 198 reaction through ab initio calculations, obtaining a

Table 1
Experimental conditions.

Set	H_2S (ppm)	O_2 (ppm)	λ
1	476	225	0.32
2	509	750	0.98
3	485	900	1.24
4	482	1500	2.07
5	492	3750	5.08
6	514	15000	19.46

rate constant of $1.5 \cdot 10^5 \cdot \text{T}^{2.1} \cdot e^{(-11,020/\text{RT})}$ (cal, mol, 199
 cm^3 , s). The inclusion of this reaction and cor- 200
 responding kinetic parameters in the mechanism 201
 does not have any effect in the calculations under 202
 the conditions of the present work. Freitas et al. 203
 [27] mentioned that the connection between the 204
 intermediate structures, HSOO and HSO_2 , takes 205
 place via an HSOO^* isomer in an electronic excited 206
 state. HSOO has been reported to be formed 207
 in the $\text{SH} + \text{O}_2(+\text{M}) \rightleftharpoons \text{HSOO}(+\text{M})$ reaction 208
 [26–30], while in some of these works the forma- 209
 tion of HSO_2 and HOSO was considered to 210
 be inaccessible directly from $\text{SH} + \text{O}_2$. The fate 211
 of HSOO may include dissociation to $\text{HSO} + \text{O}$, 212
 but this reaction has been reported to have a 213
 significant energy threshold [28], and thus is not 214
 competitive. Following the work of Ballester et 215
 al. [31], where they studied the $\text{SH} + \text{O}_2$ reaction 216
 through quasi-classical trajectory (QCT) methods, 217
 HSOO may be considered to isomerize to HSO_2 . 218
 Taking into account the barrier for HSO_2 forma- 219
 tion determined by Freitas et al. [27], we assume an 220
 activation energy of 21.3 kcal/mol for the HSOO 221
 to HSO_2 isomerization. In this work, a reaction 222
 rate of $10^{17} \cdot e^{(-21,300/\text{RT})}$ (cal, mol, cm^3 , s) has been 223
 proposed for this reaction. The impact of this 224
 assumption will be discussed later. 225

4. Results and discussion 226

The study of H_2S oxidation in a tubular flow 227
 reactor at atmospheric pressure from fuel-lean to 228
 fuel-rich conditions, in the temperature range of 229
 700–1400 K, has been carried out. The experimen- 230
 tal conditions are listed in Table 1. The influence 231
 of the amount of oxygen available on the process 232
 was studied for different values of λ , defined as 233
 $\text{O}_2(\text{real})/\text{O}_2(\text{stoichiometric})$. For an inlet total flow 234
 rate of 1 L (STP)/min, the gas residence time in the 235
 reactor varies in the 0.14–0.24 s range. 236

For the conditions listed in Table 1, the con- 237
 centrations of H_2S , SO_2 and H_2 obtained as a 238
 function of temperature are presented in Fig. 1. 239
 Symbols represent experimental data and lines 240
 model predictions using the mechanism com- 241
 piled in this work. As seen, modeling predic- 242
 tions agree fairly well with the experimental data. 243
 Additionally, experimental sulfur mass balances 244

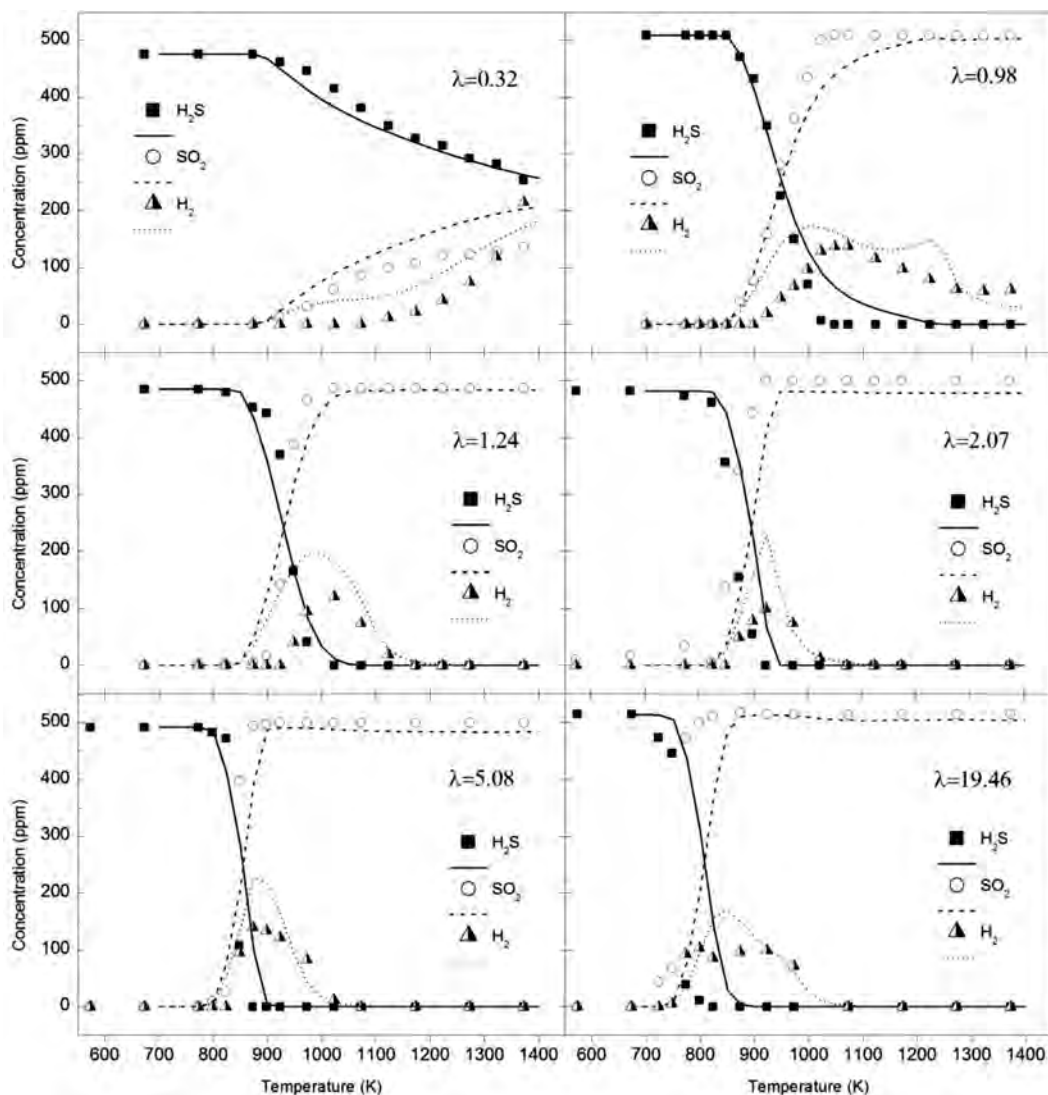


Fig. 1. Experimental results from H₂S oxidation in conditions of sets 1–6 in Table 1. Symbols represent experimental data and lines model predictions.

are shown in the supplementary material (Fig. S1), being close to 100% ($\pm 5\%$) in most cases.

Hydrogen sulfide starts to react at 925 K under reducing conditions ($\lambda = 0.32$), with lower temperatures for the onset of H₂S consumption as the stoichiometry increases, dropping to 700 K for the highest oxygen concentration used ($\lambda = 19.46$). The onset of H₂S conversion is coincident with the onset for hydrogen and sulfur dioxide formation. H₂S is fully converted into SO₂ at high temperatures, except for the case of $\lambda = 0.32$, due to the lack of oxygen. Such a result was also observed in [32], where

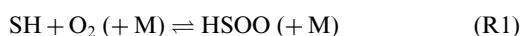
H₂S was neither consumed by the oxygen available nor by thermolysis. Under similar experimental conditions ($O_2/H_2S = 0.35$, 1375 K, $t_r = 150$ ms), but using 10% H₂S, Palma et al. [32] obtained 70% of H₂S conversion versus our 52% ($O_2/H_2S = 0.47$, 1375 K, $t_r = 140$ ms, 0.05% H₂S).

For $\lambda \geq 1$, when almost all H₂S is converted to SO₂, the H₂ formed starts to vanish. This was also observed by Zhou et al. [11], who mentioned that H₂ selectivity presents a maximum with the last traces of H₂S. The two maxima, observed for $\lambda = 0.98$ in H₂ predictions, are found to occur in the modeling by the concurrent formation and

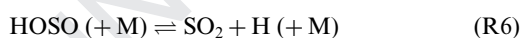
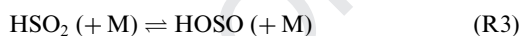
271 consumption of H₂. Hydrogen is formed mainly
272 from H₂S and consumed by reaction with O/OH
273 radicals. Once H₂S is fully consumed, the H₂ levels
274 start to decrease at high temperatures.

275 A diagram showing the main reaction pathways
276 is described in Fig. S2 of the supplementary material.
277 Solid lines represent reaction paths at all stoichiometries,
278 with the important species connected
279 by thick arrows, and dashed lines correspond to additional
280 reactions important only under reducing conditions. The most
281 relevant pathways for H₂S oxidation show that the addition
282 and modification of the reactions made in this work have a
283 significant relevance in the oxidation behavior.

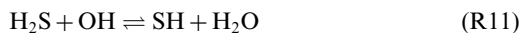
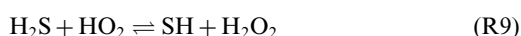
285 Calculations indicate that H₂S reacts with the
286 radical pool (H, OH and HO₂), but primarily with
287 H radicals, to rapidly form SH, independently of
288 the stoichiometry. SH continues the reaction with
289 O₂ to form mainly HSOO (R1), which isomerizes
290 to HSO₂ (R2).



291 Then, HSO₂ is branched to HOSO (R3) or to
292 the final product SO₂ through (R4) and (R5), this
293 last one under highly oxidizing conditions. HOSO,
294 as well as HSO₂, can dissociate or react with oxygen
295 (R6, R7). The reaction paths with S, SO and HS₂
296 radicals are quite similar to the ones identified by
297 Zhou et al. [11], but less important in the present
298 mechanism.

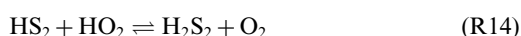
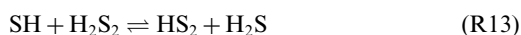


299 The reaction process is maintained primarily by
300 cause of H radicals released in the final step (R4),
301 which maintain the consumption of H₂S through
302 (R8), together with HO₂ radicals formed in (R7),
303 which react with H₂S through (R9). Reaction (R9)
304 becomes more important as the oxygen concentration
305 increases, due to the major occurrence of (R5)
306 and the increase in HO₂ concentration. The H₂O₂
307 radicals formed in (R9) decompose to OH radicals
308 through (R10), promoting H₂S consumption
309 through (R11).



The production of HO₂ radicals through (R5)
and (R7) makes reactions with this kind of radicals
to become important, as for example (R9),
which was found, together with (R2), to be the most
sensitive under our experimental conditions at all
stoichiometries. Figure S3 in the supplementary
material shows, as an example, the sensitivity analysis
for SO₂, obtained for λ = 5.08 at 823 K. Calculations
indicate that the results are sensitive to the
SH + H₂O₂ ⇌ H₂S + HO₂ reaction (-R9), which
appears always as one of the top five most sensitive
reactions. Therefore, we can confirm the necessity
of having a good determination of the kinetic parameters
of this reaction for an accurate modeling description.
Results are also sensitive to the HSOO ⇌ HSO₂
reaction (R2), which has been proposed to occur
and is included in the present mechanism. The impact
of modifying the rate for (R2) is shown in Figs. S4
and S5 of the SM. Calculations indicate the necessity
of including reaction (R2) in the model, even though
the impact of varying the rate for (R2) is appreciable
but not very significant.

Under reducing conditions, the consumption
of H₂S follows the main reaction paths discussed
in previous paragraphs. However, due to the lack of
oxygen, other important species, such as H₂S₂,
HS₂ and S₂, can be formed. S₂ can be produced
through the sequence of reactions with SH (R12-
R15), which self-reacts (R12) and forms HS₂, as
well as with H₂S₂ (R13) formed by (R14). Finally,
the HS₂ radical converts to S₂ through (R15). In
the experiment carried out in the present work under
reducing conditions, λ = 0.32, a yellow deposit
was seen at the outlet of the reactor. In this experiment,
for high temperatures, the mass balance for sulfur,
which is calculated by adding the concentrations of
H₂S and SO₂ measured at the reactor outlet, did not
close, Fig. S1. Such unbalance can be explained by
the presence of the yellow deposit, presumably S₂.
The apparition of this deposit was also previously
mentioned by Zhou et al. [11] and was attributed to
the formation of S₂ in the gas phase, which condenses
when exhaust gases are quenched.



In order to evaluate the model compiled in this
work, we have performed simulations of literature
results. In particular, we have simulated the flow
reactor results from Song et al. [12] and Gersen et
al. [19] of H₂S conversion at high pressures, where
HO₂ radicals are important, and thus the impact of

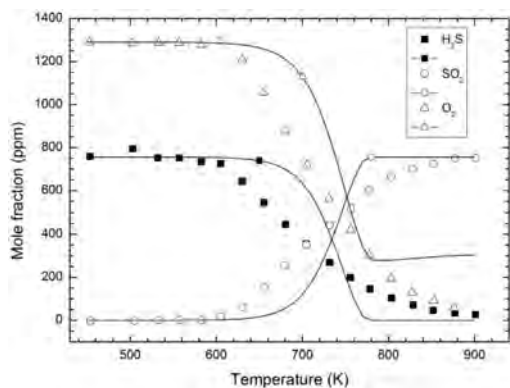


Fig. 2. Comparison of experimental data (symbols) of Song et al. [12] and simulations (lines) with the model developed in the present work. Stoichiometric conditions at 30 bar. Inlet composition: 756 ppm H₂S, 1290 ppm O₂, balance N₂ ($\lambda = 1.14$). The residence time in the isothermal zone is calculated from τ_r (s) = 3520/T (K).

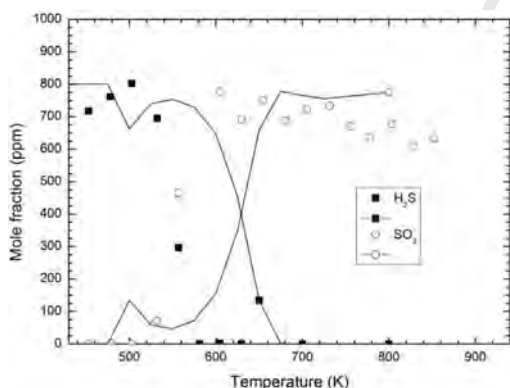


Fig. 3. Comparison of experimental data (symbols) of Song et al. [12] and simulations (lines) with the model developed in the present work. Oxidizing conditions at 30 bar. Inlet composition: 801 ppm H₂S, 4.4% O₂, balance N₂ ($\lambda = 36$). The residence time in the isothermal zone is calculated from τ_r (s) = 3100/T (K).

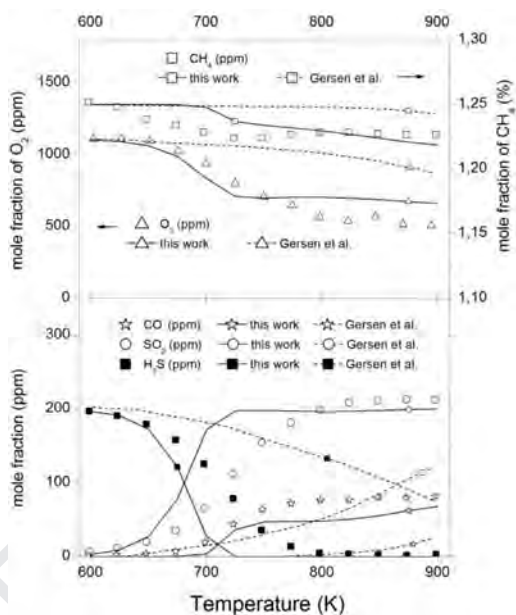
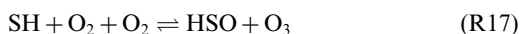
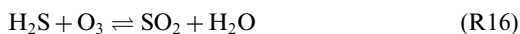


Fig. 4. Comparison between experimental data of Gersen et al. [19] (symbols) and model predictions (lines). Experiments with CH₄/H₂S in a flow reactor at 50 bar. Inlet composition: 1.25% CH₄, 1110 ppm of O₂, 200 ppm of H₂S, and balance N₂. The gas residence time is calculated as τ_r (s) = 5990/T (K).

360 (-R9) and its rate estimation may potentially be im-
 361 portant. The simulation results are shown in Figs. 2
 362 and 3 for the experiments of Song et al. [12] (stoi-
 363 chiometric and oxidizing conditions at 30 bar), and
 364 in Fig. 4 for the experiment of Gersen et al. [19] of
 365 H₂S/CH₄ oxidation (reducing conditions at 50 bar).
 366 In general, the present model reproduces well the
 367 main trends, and actually improves the previous
 368 predictions of the experimental results. The present
 369 simulation results are very similar to those obtained
 370 by Song et al. [12] under stoichiometric conditions,
 371 meanwhile, under oxidizing conditions, the authors
 372 were able to approximate the simulation results to

experimental ones by suppressing two reactions invol-
 373 ving O₃ (R16 the most important one and R17),
 374 proposed by Mousavipour et al. [33]. The model
 375 in the present work keeps these reactions, which
 376 are found to be indeed important under the experi-
 377 mental conditions of Song et al. [12]. Reaction
 378 (R17) is a source of ozone and H₂S consumes
 379 it through (R16). Despite the scatter in the experi-
 380 mental SO₂ concentrations reported by Song et al.
 381 [12], the main trends in SO₂ evolution can be
 382 seen. Although, the simulation in Fig. 3 is 50 K
 383 shifted to higher temperatures compared to the ex-
 384 perimental results, it is worthwhile to mention that
 385 the mechanism is able to reproduce the diminution
 386 in the observed H₂S mole fraction (ca. 480 K). Cal-
 387 culations indicate that the mentioned decrease be-
 388 tween approximately 480 and 540 K occurs through
 389 the interaction between H₂S and O₃ (R16), which
 390 is the dominant consumption reaction of H₂S at
 391 these temperatures. Above 500 K, reaction (R16)
 392 becomes less important because of the decrease in
 393 the O₃ concentration, and H₂S conversion proceeds
 394 mainly through reaction (R9).
 395



396 **Figure 4** includes the simulation results of both
 397 the model of Gersen et al. [19] and the present
 398 model at 50 bar. Simulation of the combustion be-
 399 havior of CH₄/H₂S and formation of products is
 400 improved with the present mechanism, which pre-
 401 dicted well the tendencies. Under these conditions,
 402 H₂S reacts to SO₂ through the SH reaction chan-
 403 nel (R1 and R2). In the case of CH₄/H₂S oxida-
 404 tion, the model predicts that CO starts to be formed
 405 when H₂S is almost consumed, although experi-
 406 mentally this happens earlier. This might be due to
 407 the lack of reactions in the present mechanism de-
 408 scribing the interaction between CH₄ and H₂S or to
 409 a non appropriate value for the kinetic parameters
 410 of the reaction of H₂S with the CH₃OO peroxide,
 411 which were estimated to be the same as in the re-
 412 verse H₂S + HO₂ reaction (-R9) by Zhou et al. [11],
 413 and mentioned by the authors to be important [19].

414 5. Conclusions

415 Oxidation of H₂S at atmospheric pressure has
 416 been studied under different reaction atmospheres,
 417 varying the air excess ratio (λ) from reducing
 418 ($\lambda = 0.32$) to oxidizing conditions ($\lambda = 19.46$). The
 419 experiments were carried out in a tubular flow reac-
 420 tor, in the 700–1400 K temperature range and con-
 421 centrations of H₂S, SO₂ and H₂ were determined.
 422 A detailed kinetic mechanism for the conversion of
 423 H₂S under the present conditions has been devel-
 424 oped, evidencing the importance of given reactions,
 425 like the interaction of SH radicals with the radical
 426 pool and oxygenated species, such as O₂ and H₂O₂.
 427 This mechanism has been used to simulate the ex-
 428 perimental results obtained in the present work, to-
 429 gether with data from the literature, obtaining a
 430 fairly good agreement under the different condi-
 431 tions. The changes in the mechanism included the
 432 addition of reaction (HSOO \rightleftharpoons HSO₂), supported
 433 by recent theoretical works, as a key step in a faster
 434 reaction path of SH oxidation, and modification
 435 of (SH + H₂O₂ = H₂S + HO₂) kinetic parameters,
 436 which has a significant impact on the reaction path-
 437 ways of H₂S oxidation. The main reactions gov-
 438 erning the conversion of H₂S have been identified,
 439 together with the necessity for a better determina-
 440 tion of the kinetic parameters of important reac-
 441 tions, including the isomerization of HSOO into
 442 HSO₂ and the interaction of H₂S with HO₂. This
 443 work supports the evolution of SH + O₂ reaction
 444 through HSOO to HSO₂ isomerization.

445 Acknowledgments

446 The authors express their gratitude to Aragón
 447 Government and European Social Fund (GPT
 448 group), and to MINECO and FEDER (Project
 449 CTQ2015-65226 and grant BES-2016-076610) for
 450 financial support.

Supplementary materials

451

Supplementary material associated with this arti-
 cle can be found, in the online version, at doi:10.
 1016/j.proci.2018.05.005.

452

453

454

REFERENCES

455

- [1] M. Binoist, B. Labégorre, F. Monnet, et al., *Ind. Eng. Chem. Res.* 42 (2003) 3943–3951. 456
- [2] T.Y. Cong, A. Raj, J. Chanaphet, S. Mohammed, S. Ibrahim, A. Al Shoaibi, *Int. J. Hydrogen Energy* 41 (2016) 6662–6675. 457
- [3] W.D. Monnery, K.A. Hawboldt, A. Pollock, W.Y. Svrcek, *Chem. Eng. Sci.* 55 (2000) 5141–5148. 458
- [4] US Department of Energy, *Report of Basic Research Needs for Clean and Efficient Combustion of 21st Century Transportation Fuels*, US Department of Energy, 2006. 459
- [5] W.C. Gardiner, *Gas-phase Combustion Chemistry* (Ed.), Springer, New York, 2000. 460
- [6] D. Bongartz, A.F. Ghoniem, *Combust. Flame* 162 (2015) 544–553. 461
- [7] C.F. Cullis, M.F.R. Mulcahy, *Combust. Flame* 18 (1972) 225–292. 462
- [8] R. Pahl, K. Holtappels, *Chem. Eng. Technol.* 28 (2005) 746–749. 463
- [9] M. Frenklach, J.H. Lee, J.N. White, W.C. Gardiner, *Combust. Flame* 41 (1981) 1–16. 464
- [10] H. Selim, S. Ibrahim, A. Al Shoaibi, A.K. Gupta, *Appl. Energy* 113 (2014) 1134–1140. 465
- [11] C.R. Zhou, K. Sendt, B.S. Haynes, *Proc. Combust. Inst.* 34 (2013) 625–632. 466
- [12] Y. Song, H. Hashemi, J.M. Christensen, C. Zou, B.S. Haynes, P. Marshall, P. Glarborg, *Int. J. Chem. Kinet.* 49 (2017) 37–52. 467
- [13] M.U. Alzueta, R. Bilbao, M. Finestra, *Energy Fuels* 15 (2001) 724–729. 468
- [14] M.U. Alzueta, R. Bilbao, P. Glarborg, *Combust. Flame* 127 (2001) 2234–2251. 469
- [15] M. Abián, Á. Millera, R. Bilbao, M.U. Alzueta, *Fuel* 159 (2015) 550–558. 470
- [16] M. Abián, M. Cebrián, Á. Millera, R. Bilbao, M.U. Alzueta, *Combust. Flame* 162 (2015) 2119–2127. 471
- [17] CHEMKIN-PRO 15131, Reaction Design, 2013. 472
- [18] A. Mellouki, A.R. Ravishankara, *Int. J. Chem. Kinet.* 26 (1994) 355–365. 473
- [19] S. Gersen, M. van Essen, H. Darneveil, et al., *Energy Fuels* 31 (2017) 2175–2182. 474
- [20] O. Mathieu, F. Deguillaume, E.L. Petersen, *Comb. Flame* 161 (2014) 23–36. 475
- [21] R.R. Friedl, W.H. Brune, J.G. Anderson, *J. Phys. Chem.* 89 (1985) 5505–5510. 476
- [22] M. Batiha, M. Altarawneh, M. Al-Harashsheh, I. Altarawneh, S. Rawadieh., *Comput. Theor. Chem.* 970 (2011) 1–5. 477
- [23] K. Tsuchiya, K. Kamiya, H. Matsui, *Int. J. Chem. Kinet.* 29 (1997) 57–66. 478
- [24] F.G. Cerru, A. Kronenburg, R.P. Lindstedt, *Combust. Flame* 146 (2006) 437–455. 479
- [25] R.A. Stachnik, M.J. Molina, *J. Phys. Chem.* 91 (1987) 4603–4606. 480
- [26] J.D. Garrido, M.Y. Ballester, Y. Orozco-González, S. Canuto, *J. Phys. Chem. A* 115 (2011) 1453–1461. 481

512

- 513 [27] G.N. Freitas, J.D. Garrido, M.Y. Ballester, 521
514 M.A.C. Nascimento, *J. Phys. Chem. A* 116 (2012) 522
515 7677–7685. 523
- 516 [28] A. Goumri, J.-D.R. Rocha, D. Laakso, C.E. Smith, 524
517 P. Marshall, *J. Phys. Chem. A* 103 (1999) 11328– 525
518 11335. 526
- 519 [29] A. Goumri, D. Laakso, J.D.R. Rocha, C.E. Smith, 527
520 P. Marshall, *J. Chem. Phys.* 102 (1995) 161–169. 528
- [30] C. Zhou, K. Sendt, B.S. Haynes, *J. Phys. Chem. A* 521
113 (2009) 2975–2981. 522
- [31] M.Y. Ballester, Y.O. Guerrero, J.D. Garrido, *Int. J.* 523
Quantum Chem. 108 (2008) 1705–1713. 524
- [32] V. Palma, V. Vaiano, D. Barba, et al., *Int. J. Hydrog.* 525
Energy 40 (2015) 106–113. 526
- [33] S.H. Mousavipour, M. Mortazavi, O. Hematti, *J.* 527
Phys. Chem. A 117 (2013) 6744–6756. 528